

ORIGINAL RESEARCH ARTICLE

Exact analysis of MHD Walters'-B fluid flow with non-singular fractional derivatives of Caputo-Fabrizio in the presence of radiation and chemical reaction

Muhammad Asjad Imran*, Maryam Aleem, M. Bilal Riaz

Department of Mathematics, University of Management and Technology, Lahore 54700, Pakistan

* Corresponding author: Muhammad Asjad Imran, imran.asjad@umt.edu.pk

ABSTRACT

The present article reports the applications of Caputo-Fabrizio time-fractional derivatives. This article generalizes the idea of unsteady MHD free convective flow in a Walters.-B fluid with heat and mass transfer study over an exponential isothermal vertical plate embedded in a porous medium. The governing equations are converted into dimensionless form and extended to fractional model. The generalized Walters-B fluid model has been solved analytically using the Laplace transform technique. From the general solutions we reduce limiting solutions when to the similar motion for Newtonian fluid. The corresponding expressions for and Nusselt and Sherwood numbers are also assessed. Numerical results for velocity, temperature and concentration are demonstrated graphically for various factors of interest and discussed. As a result, we have plotted the influence of fractional parameter on fluid flow and drawn comparison between fractional Walters'-B and fractional Newtonian fluid and found that fractional Newtonian fluid is faster than fractional Walters'-B fluids.

Keywords: free convection; mass and heat transfer; chemical reaction; Caputo-Fabrizio time derivative; radiation; MHD

ARTICLE INFO

Received: 10 October 2019
Accepted: 13 November 2019
Available online: 16 December 2019

COPYRIGHT

Copyright © 2019 by author(s).
Journal of Polymer Science and Engineering
is published by EnPress Publisher LLC. This
work is licensed under the Creative Commons
Attribution-NonCommercial 4.0 International
License (CC BY-NC 4.0).
<https://creativecommons.org/licenses/by-nc/4.0/>

1. Introduction

For a long period the fractional calculus, that has derivatives and integrals of non-natural degree, was originated as a purely theoretic domain^[1,2]. Recently, it's been depicted that it could be used to explicate certain tangible problems, and likewise for procedures where memory upshots are crucial^[3]. In this way, although the classical derivative establishes the instantaneous modification of a function, the parameter of the fractional derivative can be inferred as a memory indicator of the fluctuation of the function, allowing the former instants. Referable to this understanding, in last years, fractional calculus bears productively implemented to dissimilar areas^[4,5]. It's also concerning to observe a few modern works in order to find appropriate fractional analogues of the so-called particular functions^[6-8]. There are several definitions—Riemann, Liouville, Caputo, Grunwald-Letnikov, Marchaud, Weyl, Riesz, Feller, and others- for fractional derivatives and integrals, (see e.g., [1,2,9,10] and references therein). These diverseness of definitions flows from the fact that fractional operators acquire a different kernel representations in different function spaces. In a recent work Caputo and Fabrizio^[11] preceded a new fractional derivative, analysis, e.g., in Losada and Nieto's study^[12].

Magnetohydrodynamic (MHD) flows of acquitting fluids stimulated because of buoyancy effects originating from density fluctuations in the gravitational domain are found in several natural phenomena and technological arrangements. If fluent is incompressible then the density fluctuation owed to vary in pressure is minimal. All the same, the density variation referable to inhomogeneous inflaming and l chemical reaction can't be ignored as this is responsible for innate convection. Probe of interaction of international enforced magnetic flux to the natural convection boundary layer streams of an electrically acquitting liquid is significant as a drag force stimulated due to enforced magnetic field named Lorentz force and this force is moderating the fluid flow rate. Such fluent flows might incur diligences in numerous industries and technical organizations like metrology, chemical manufactures, electrical power propagation, solar energy generation, atomic directing, boundary layer assure in polymer treating and aerodynamics etcetera. Due to diverse applications of MHD boundary layer flows of conducting fluids a lot of investigators have enquired the tempt of magnetic field on hydromagnetic currents^[13-23]. If a partly ionized fluent with low density (plasma) is interacted with a substantial magnetic field the phenomena of Hall and ion-slip effects inherit the characterization and for specified fluids the inducted electric current (Hall and ion-slip currents) is admitted in generalized Ohm's law for a proceeding conductor^[24].

In all of these research probes fluid is counted to be Newtonian. However, the dynamics of non-Newtonian fluid is considered significantly as it has general applications in plastic fabricating procedure, execution of paints and lubricators, food preserving and in geophysical and biological fluids. Viscoelastic fluid is one of the sub-categories of non-Newtonian fluid. Beard and Walters^[25] have portrayed a classical research paper on the two-dimensional stagnation point flow of the elastico-viscous fluid. The model demonstrated in this paper is titled as Walters'-B fluid model and this model opened the new scope for the technologists and engineers to analyze the dynamics of viscoelastic fluids. Propelled from the diverse progressive and engineering applications, latterly many extensive research probes have been demonstrated by the researchers^[26-35] to canvas the dynamics of viscoelastic fluid by applying respective computational and analytical techniques. Influence of magnetic field on elastic viscous fluid is studied significantly due to its various applications in many fields of scientific discipline and applied science, in particular, in geophysical science, fluid engineering, and petroleum and chemical engineering. Hayat et al.^[30] portrayed an analytical bailiwick on hydromagnetic oscillating flow of a rotating second grade fluid bounded by poriferous plate using Laplace transform method. Siddheshwar and Mahabaleshwar^[31] canvassed MHD flow of a viscoelastic liquid and heat transfer over a stretching sheet with radiation and heat source. Ghasemi et al.^[32] discussed heat carry-over features of viscoelastic MHD flow of Walters'-B fluid over a non-isothermal unfolding sheet. Prakash et al.^[33] examined heat transfer features of MHD flow of soiled viscoelastic fluid through poriferous medium by reckoning variable viscosity.

The present article studies the applications of Caputo-Fabrizio time-fractional derivatives. This article also generalizes the theme of unsteady MHD free convective flow in a Walters.-B fluid with heat transfer analysis across an exponential isothermal vertical plate embedded in a poriferous medium. The classical model for Walters'-B fluid is expressed in dimensionless form with the help of non-dimensional variables. Moreover, the dimensionless model is converted into a fractional model named as a generalized Walters.-B fluid model. The governing equations of generalized Walters'-B fluid model have been worked out analytically by applying the Laplace transform method. They satisfy all levied initial and boundary conditions and for $\Gamma \rightarrow 0$ can be reduce to the similar results for Newtonian fluids. The corresponding expressions for skin friction and Nusselt number are also assessed. Numerical results for velocity and temperature are displayed graphically for several parameters of interest and talked about. This study is of cardinal importance and frequently originates in many practical situations such as chemical engineering and polymer extrusion procedures.

2. Statement of the problem

Consider the unsteady free convective flow of an electrically conducting, incompressible non-Newtonian Walters'-B fluid over an upright rigid plate at $y = 0$, driven by buoyancy force due to concentration and temperature differences, occurring upward beside the plate. The x -axis is taken parallel to the plate in upward direction and y -axis is normal to plane of the plate. The flow is subject to a uniform magnetic field of strength B_0 applied normal to the plate. It is assumed that the magnetic Reynolds number is very small and the induced magnetic field is neglected. Furthermore, the electric field due to polarization of charges is negligible as there is no electric field. Initially for $t \leq 0$, both the fluid and plate are at rest and at uniform temperature T_∞ and concentration C_∞ . After time $t > 0$, the plate starts to accelerate in its own plane with exponential acceleration and the concentration and temperature level are lowered or raised to $T_\infty + \frac{U_0^2}{\nu}(T_w - T_\infty)t$ and $C_\infty + \frac{U_0^2}{\nu}(C_w - C_\infty)$. Also set of governing equation is given under the usual Boussineq's approximation as

$$\frac{\partial u(y, t)}{\partial t} = \nu \frac{\partial^2 u(y, t)}{\partial y^2} - \frac{k_o}{\rho} \frac{\partial^3 u(y, t)}{\partial t \partial y^2} - \frac{\sigma B_0^2}{\rho} u(y, t) + g\beta_T(T(y, t) - T_\infty) + g\beta_C(C(y, t) - C_\infty) \quad (1)$$

$$\rho c_p \frac{\partial T(y, t)}{\partial t} = k \frac{\partial^2 T(y, t)}{\partial y^2} - \frac{\partial q_r}{\partial y} \quad (2)$$

$$\frac{\partial C(y, t)}{\partial t} = D \frac{\partial^2 C(y, t)}{\partial y^2} - K[C(y, t) - C_\infty] \quad (3)$$

With initial and boundary conditions

$$\begin{aligned} u(y, 0) = 0, T(y, 0) = T_\infty, C(y, 0) = C_\infty, \\ u(0, t) = U_0 e^{at}, T(0, t) = T_\infty + \frac{U_0^2}{\nu}(T_w - T_\infty)t, C(0, t) = C_\infty + \frac{U_0^2}{\nu}(C_w - C_\infty)t, t > 0, \\ u(y, t) \rightarrow 0, T(y, t) \rightarrow 0, C(y, t) \rightarrow 0, \text{ as } y \rightarrow \infty \end{aligned} \quad (4)$$

Introducing non-dimensional variables into Equations (1)–(4).

$$\left. \begin{aligned} y^* = \frac{U_0}{\nu} y, t^* = \frac{U_0^2}{\nu} t, u^* = \frac{u}{U_0}, T^* = \frac{T - T_\infty}{T_w - T_\infty}, C^* = \frac{C - C_\infty}{C_w - C_\infty}, \\ K^* = \frac{\nu}{U_0^2} K, a^* = \frac{\nu}{U_0^2} a. \end{aligned} \right\} \quad (5)$$

Dropping out the star notation, our problem reduces to the set of following dimensionless partial differential equations

$$\frac{\partial u(y, t)}{\partial t} = \frac{\partial^2 u(y, t)}{\partial y^2} - \Gamma \frac{\partial^3 u(y, t)}{\partial t \partial y^2} - Mu(y, t) + T(y, t) + NC(y, t) \quad (6)$$

$$Pr_{eff} \frac{\partial T(y, t)}{\partial t} = \frac{\partial^2 T(y, t)}{\partial y^2} \quad (7)$$

$$\frac{\partial C(y, t)}{\partial t} = \frac{1}{Sc} \frac{\partial^2 C(y, t)}{\partial y^2} - KC(y, t) \quad (8)$$

$$\left. \begin{aligned} u(y, 0) = 0, T(y, 0) = 0, C(y, 0) = 0, y \geq 0, \\ u(0, t) = \exp(at), T(0, t) = t, C(0, t) = t, t > 0, \\ u(y, t) \rightarrow 0, T(y, t) \rightarrow 0, C(y, t) \rightarrow 0, \text{ as } y \rightarrow \infty. \end{aligned} \right\} \quad (9)$$

To obtain a model with fractional derivative replace integer derivative of order one with non-integer order α .

$$D_t^\alpha u(y, t) = \frac{\partial^2 u(y, t)}{\partial y^2} - \Gamma D_t^\alpha \frac{\partial^2 u(y, t)}{\partial y^2} - Mu(y, t) + T(y, t) + NC(y, t) \quad (10)$$

$$Pr_{eff} D_t^\alpha T(y, t) = \frac{\partial^2 T(y, t)}{\partial y^2} \quad (11)$$

$$D_t^\alpha C(y, t) = \frac{1}{Sc} \frac{\partial^2 C(y, t)}{\partial y^2} - KC(y, t) \quad (12)$$

where Caputo-Fabrizio time-fractional derivative^[11] is define by

$$D_t^\alpha u(y, t) = \frac{1}{1-\alpha} \int_0^t \exp\left(\frac{-\alpha(t-\tau)}{1-\alpha}\right) \frac{\partial u(y, \tau)}{\partial \tau} d\tau, \quad 0 \leq \alpha < 1 \quad (13)$$

3. Solution of the problem

3.1. Temperature field for $0 < \alpha < 1$

Applying Laplace transform to equation Equation (11) and using Equation (9), we get

$$\frac{\partial^2 \bar{T}(y, q)}{\partial y^2} - \frac{Pr_{eff} q}{(1-\alpha)q + \alpha} \bar{T}(y, q) = 0 \quad (14)$$

satisfy the conditions

$$\bar{T}(y, q) = \frac{1}{q^2}, \bar{T}(y, q) \rightarrow 0, \text{ as } y \rightarrow \infty \quad (15)$$

Solution of Equation (14) subject to Equation (15) is as follow

$$\bar{T}(y, q) = \frac{1}{q} * \frac{1}{q} e^{-y \sqrt{\frac{Pr_{eff} q}{(1-\alpha)q + \alpha}}} \quad (16)$$

Applying inverse Laplace transform to Equation (16) by using (A10) as well as convolution theorem, we get

$$T(y, t) = \int_0^t H(t-\tau) \left(1 - \frac{2Pr_{eff}}{\pi} \int_0^\infty \frac{\sin\left(\frac{y}{\sqrt{1-\alpha}}x\right)}{x(Pr_{eff} + x^2)} e^{\left(\frac{-\alpha}{1-\alpha}\tau x^2\right)} dx \right) d\tau \quad (17)$$

3.1.1. Nusselt number for $0 < \alpha < 1$

Heat transfer rate from plate to the fluid in terms of Nusselt number can be obtained by using the following expression and expressed in terms of generalized G-function.

$$Nu = -\left. \frac{\partial T(y, t)}{\partial y} \right|_{y=0} = \sqrt{Pr_{eff} \gamma} G_{1, -\frac{3}{2}}(-\alpha \gamma, t) \quad (18)$$

3.1.2. Temperature field for $\alpha \rightarrow 1$

For $\alpha \rightarrow 1$ in Equation (16), the expression for temperature is given as

$$T(y, t) = \int_0^t H(t-\tau) \operatorname{erfc}\left(\frac{y\sqrt{Pr_{eff}}}{2\sqrt{\tau}}\right) d\tau \quad (19)$$

3.1.3. Nusselt number for $\alpha \rightarrow 1$

$$Nu = -\frac{\partial T(y, t)}{\partial y} \Big|_{y=0} = \sqrt{Pr_{eff} R_{\frac{3}{2}, 0}}(0, 0, t) \quad (20)$$

3.2. Species concentration for $0 < \alpha < 1$

Applying the Laplace transform to Equation (13) and using Equation (9) the, we find that

$$\bar{C}(y, q) = \frac{1}{q^2} e^{-y\sqrt{Sc}} \sqrt{\frac{q+b}{q+a_1}}, b = \frac{K\alpha\gamma}{\gamma Sc + K} \text{ and } a_1 = \alpha\gamma \quad (21)$$

To obtain inverse Laplace of Equation (21), in more suitable form

$$\bar{C}(y, q) = \frac{q+a}{q^2} * \frac{e^{-y\sqrt{Sc}} \sqrt{\frac{q+b}{q+a_1}}}{q+a} \quad (22)$$

Applying inverse Laplace transform to Equation (21)

$$C(y, t) = \int_0^t (H(t-\tau) + a(t-\tau)) e^{-a\tau-y} d\tau - \frac{y\sqrt{b-a_1}}{2\sqrt{\pi}} \int_0^t (H(t-\tau) + a(t-\tau)) \left[\int_0^\infty \int_0^\xi \frac{e^{-a\xi}}{\sqrt{\xi}} \left(e^{a\xi-a_1\xi-\frac{y^2 Sc}{4u}-u} \right) \left(I_1 \left(2\sqrt{(b-a_1)u\xi} \right) \right) d\xi du \right] d\tau \quad (23)$$

3.2.1. Sherwood number for $0 < \alpha < 1$

Mass transfer rate from plate to the fluid in terms of Sherwood number can be obtained by using the following expression.

$$Sh = -\frac{\partial C(y, t)}{\partial y} \Big|_{y=0} = \int_0^t \frac{1}{\sqrt{a_1}} erf(\sqrt{a_1(t-\tau)}) \left[\frac{e^{-b\tau}}{\sqrt{\pi\tau}} + \frac{1}{\sqrt{b}} erf(\sqrt{b\tau}) \right] d\tau \quad (24)$$

3.2.2. Species concentration for $\alpha \rightarrow 1$

$$C(y, q) = \int_0^t H(t-\tau) \Psi(y, \tau, a, 0) d\tau \quad (25)$$

3.2.3. Sherwood number for $\alpha \rightarrow 1$

Rate of mass transfer for Walters'-B fluid is

$$Sh = -\frac{\partial C(y, t)}{\partial y} \Big|_{y=0} = \int_0^t \frac{1}{\sqrt{\gamma}} erf(\sqrt{\gamma(t-\tau)}) \left[\frac{e^{-b\tau}}{\sqrt{\pi\tau}} erf(\sqrt{b\tau}) \right] d\tau \quad (26)$$

3.3. Velocity field $0 < \alpha < 1$

Applying the Laplace transform to Equation (13) and using the corresponding initial conditions, we find that

$$\frac{\partial^2 \bar{u}(y, q)}{\partial y^2} - \frac{q + M\alpha + M(1-\alpha)q}{(1-\alpha)q + \alpha - \Gamma q} \bar{u}(y, q) = \frac{(1-\alpha)q + \alpha}{\Gamma q - (1-\alpha)q - \alpha} (\bar{T}(y, q) + N\bar{C}(y, q)) \quad (27)$$

$$\bar{u}(0, q) = \frac{1}{s-a}, \bar{u}(y, q) \rightarrow 0, \text{ as } y \rightarrow \infty \quad (28)$$

The Equation (27) is second order non-homogeneous differential equations and its solution subject to condition (28) is

$$\begin{aligned}
\bar{u}(y, q) = & \frac{1}{q-a} e^{-y \sqrt{\frac{(q+M)\gamma+Mq}{(\alpha-\Gamma q)\gamma+q}}} + \\
& + \frac{\frac{1}{q^2} (q + \alpha\gamma)^2}{Pr_{eff} q \gamma ((\Gamma q - \alpha)\gamma - q) + ((q + M\alpha)\gamma + Mq)(q + \alpha\gamma)} \left(e^{-y \sqrt{\frac{Pr_{eff} q \gamma}{q + \alpha\gamma}}} - e^{-y \sqrt{\frac{(q+M\alpha)\gamma+Mq}{(\alpha-\Gamma q)\gamma+q}}} \right) + \\
& + \frac{\frac{N}{q^2} (q + \alpha\gamma)^2}{Sc(q(\gamma + K) + K\alpha\gamma)((\Gamma q - \alpha)\gamma - q) + ((q + M\alpha)\gamma + Mq)(q + \alpha\gamma)} \cdot \\
& \cdot \left(e^{-y \sqrt{\frac{Sc(q(\gamma+K)+K\alpha\gamma)}{q+\alpha\gamma}}} - e^{-y \sqrt{\frac{(q+M\alpha)\gamma+Mq}{(\alpha-\Gamma q)\gamma+q}}} \right)
\end{aligned} \tag{29}$$

3.4. Limiting case when $\Gamma \rightarrow 0$ (viscous fluid)

$$\begin{aligned}
\bar{u}(y, q) = & \frac{1}{q-a} e^{-y \sqrt{\frac{(q+M)\gamma+Mq}{\alpha\gamma+q}}} + \\
& + \frac{\frac{1}{q^2} (q + \alpha\gamma)^2}{((q + M\alpha)\gamma + Mq)(q + \alpha\gamma) - Pr_{eff} q \gamma (\alpha\gamma + q)} \left(e^{-y \sqrt{\frac{Pr_{eff} q \gamma}{q + \alpha\gamma}}} - e^{-y \sqrt{\frac{(q+M\alpha)\gamma+Mq}{\alpha\gamma+q}}} \right) + \\
& + \frac{\frac{N}{q^2} (q + \alpha\gamma)^2}{((q + M\alpha)\gamma + Mq)(q + \alpha\gamma) - Sc(q(\gamma + K) + K\alpha\gamma)(\alpha\gamma + q)} * \\
& * \left(e^{-y \sqrt{\frac{Sc(q(\gamma+K)+K\alpha\gamma)}{q+\alpha\gamma}}} - e^{-y \sqrt{\frac{(q+M\alpha)\gamma+Mq}{\alpha\gamma+q}}} \right)
\end{aligned} \tag{30}$$

4. Numerical results and discussions

Generalized Walters'-B fluid model is being solved analytically by applying the Laplace transform method satisfying all levied initial and boundary conditions. Numerical results for velocity, concentration and temperature are showed graphically for respective parameters like effective the Prandtl number, Pr_{eff} , the magnetic field parameter M , the permeability of porous medium K , the radiation conductivity parameter Nr , the ratio of buoyancy forces N , the Schmidt number Sc , the fractional parameter α and time t .

Figure 1 is plotted to see the influence of radiation conduction parameter Nr on the temperature of Walters'-B fluid. It can be seen from the figure that by increasing the value of Nr the temperature of the fluid increases. Physically, larger the value of parameter R , the ratio of conductivity dominates across the radiation. Consequently the boundary layer thickness also increases.

Figure 2 is plotted to see the effect of fractional parameter α on temperature of Walters'-B fluid. The temperature is an increasing function of α as shown in **Figure 2**. For large values of alpha and small values of time, temperature decreases near the plate region.

Effect of Pr on the temperature is depicted in **Figure 3**. Its observable from **Figure 3** that by raising the value of Prandtl number the temperature of the fluid decreases. As expected increasing Pr reduces the thermal conduction and raises the viscosity of the fluid leads the decrease in the thickness of thermal boundary layer.

Concentration is diagrammed versus y in **Figure 4** for several fractional parameter α . It can be envisioned that by increasing the value of α concentration increases and is minimum near the plate.

Effect of parameter of permeability of porous medium K can be checked in **Figure 5** which is plotted against y by fixing the values of other parameters. It can be seen that concentration is a decreasing function of K . Effect of dimensionless Schmidt number Sc on concentration can be seen from **Figure 6**. It is evident that by increasing the value of Sc the concentration decreases which is due to the reason that for larger values of Sc molecular diffusivity decreases and it leads to decrement the boundary layer of concentration.

Variation of α on fluid's velocity is drawn in **Figure 7**. It is distinctly figured that by maximizing the value of α velocity also step-ups. It is because of the fact that by employing fractional model flow can be raised; i-e the fractional fluid has greater velocity than ordinary fluid.

Velocity of the Walter's fluid decrements by raising the value of chemical reaction parameter K , as pictured in **Figure 8**. It's distinctly showed that by increase in the value of K lead to fall in the velocity of the fluid. Magnetic field parameter M as shown in **Figure 9**. Physically it is due to the fact that drag force is effecting fluid's velocity hence opposing motion of the fluid. **Figure 10** indicates the boundary forces parameter N verses y on the velocity visibilities. It can be seen that velocity increases by increasing the values of N . The velocity is decreasing function of Sc as displayed in **Figure 11**. Physically it is due to the reason that the concentration buoyancy effect decreases by increasing the values of Sc causing a reduction in the velocity of the fluid besides the boundary layer thickness.

By increasing the value of effective Prandtl number the fluid's velocity step-downs which is due to the reason that fluid's with greater values of Prandtl number have more viscosity and less thermal conductivity, forming the fluid more denser and hence decreases fluid's velocity as shown in **Figure 12**.

Velocity is a decreasing function of Walter's parameter Γ as shown in **Figure 13**. **Figure 14** is plotted to check influence of time on fluid's velocity. It can be figured that by maximizing the value of time fluid's velocity also step-ups. **Figures 15–17** are plotted to see the substantiation of inversion algorithms. The overlapping results indicate that by applying the inversion algorithm the obtained results are same. **Figure 18** shows the comparison of fractional Walter's fluid and fractional viscous fluid. It can be experienced that fractional viscous fluid is faster than fractional Walters'-B fluid.

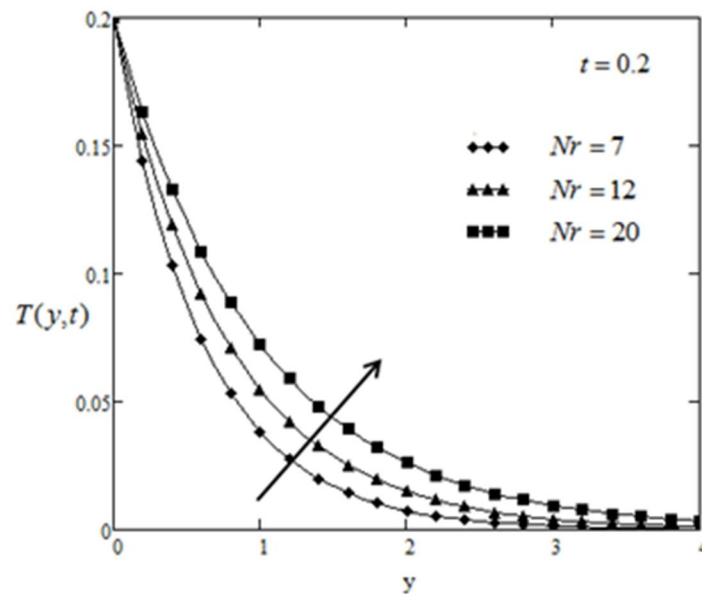


Figure 1. Temperature profile for various Nr when $\alpha = 0.5$ and $Pr = 12$.

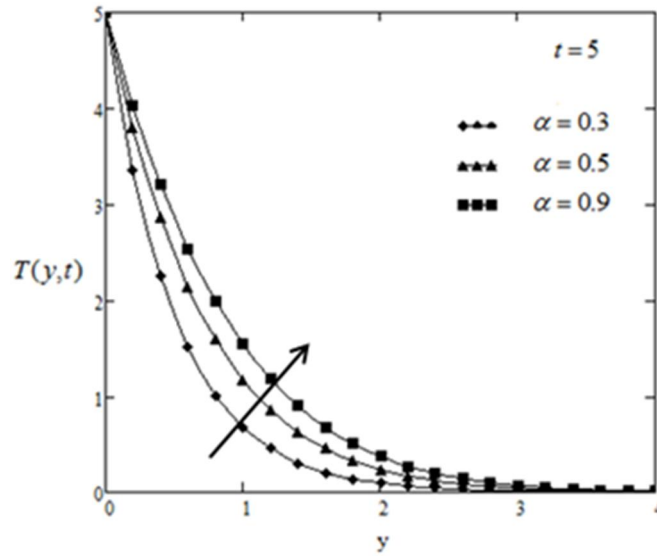


Figure 2. Temperature profile for various α when $Pr = 10$ and $Nr = 1.5$.

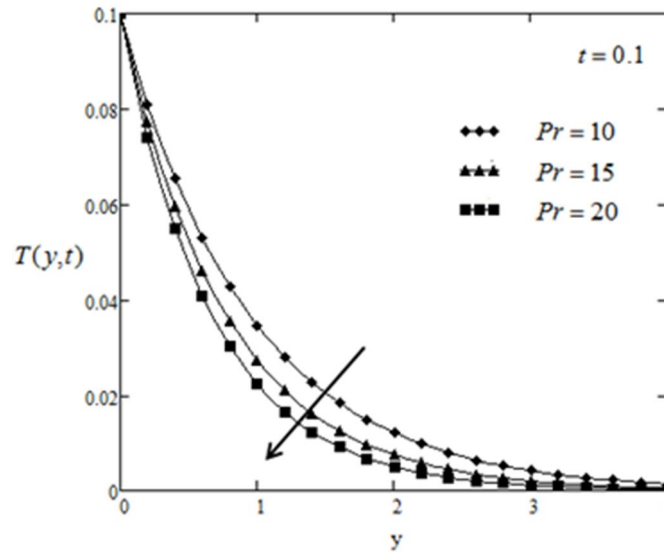


Figure 3. Temperature profile for various Pr when $Nr = 10$ and $Pr = 10$.

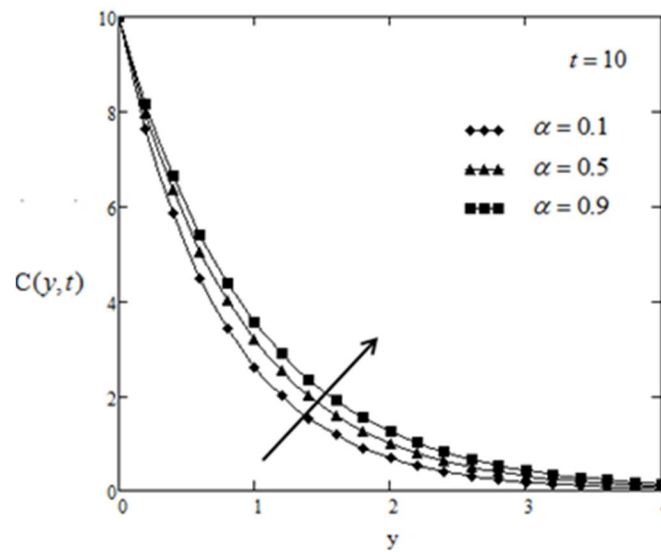


Figure 4. Concentration profile for various α when $K = 0.2$, $Sc = 2$ and $Pr = 10$.

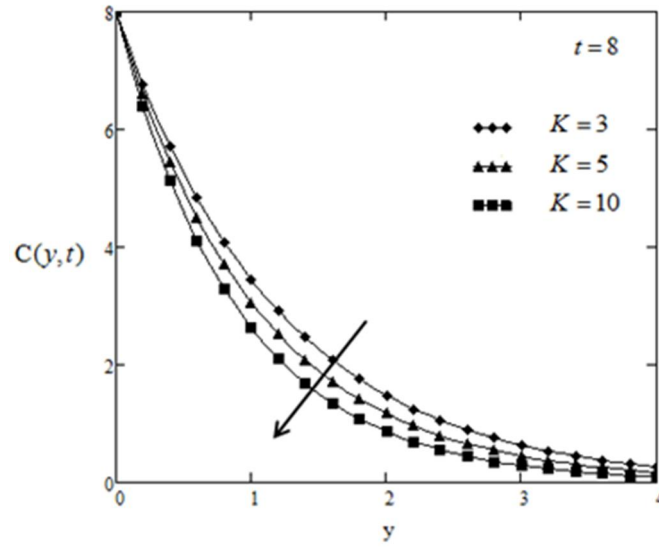


Figure 5. Concentration profile for various K when $\alpha = 0.5$, $\gamma = 3.5$, $Sc = 2$ and $Pr = 12$.

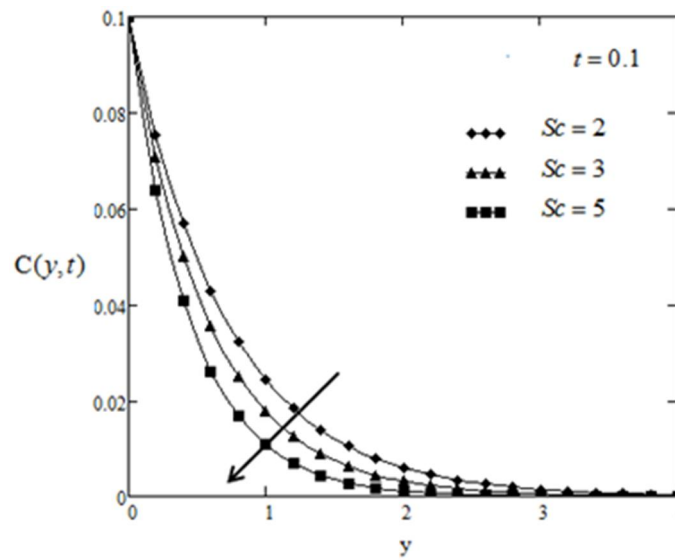


Figure 6. Concentration profile for various Sc when $\gamma = 0.1$, $\alpha = 0.1$ and $K = 0.3$.

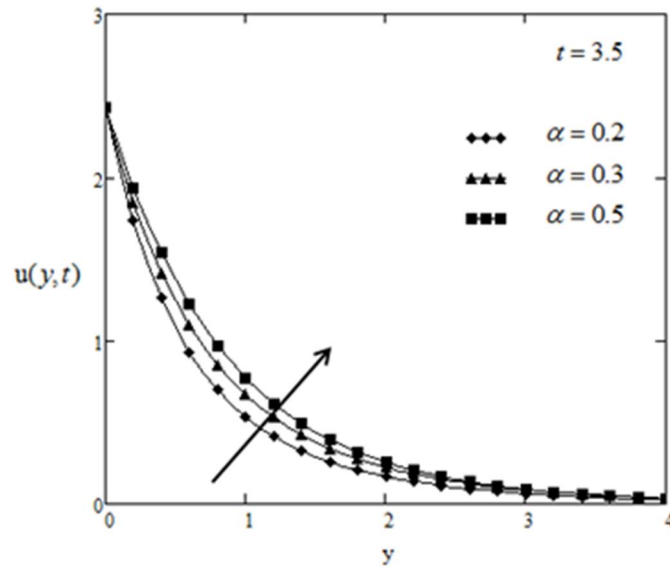


Figure 7. Velocity profile for various α when $\gamma = 0.9$, $N = 0.5$, $\Gamma = 0.3$, $Sc = 0.22$, $Pr_{eff} = 10$ and $K = 3.5$.

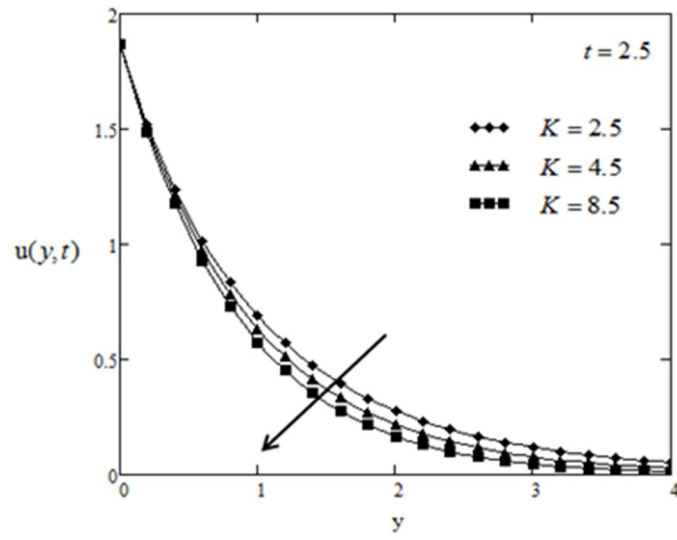


Figure 8. Velocity profile for various K when $\alpha = 0.2$, $N = 0.6$, $\Gamma = 0.4$, $Sc = 0.22$, $Pr_{eff} = 10$, $M = 1.5$ and $\gamma = 0.3$.

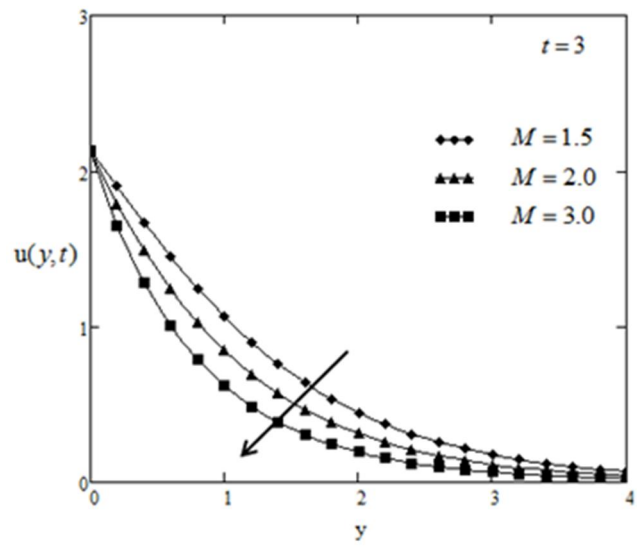


Figure 9. Velocity profile for various M when $\alpha = 0.8$, $N = 0.1$, $\Gamma = 0.2$, $Sc = 0.22$, $Pr_{eff} = 9$, $K = 1.5$ and $\gamma = 0.2$.

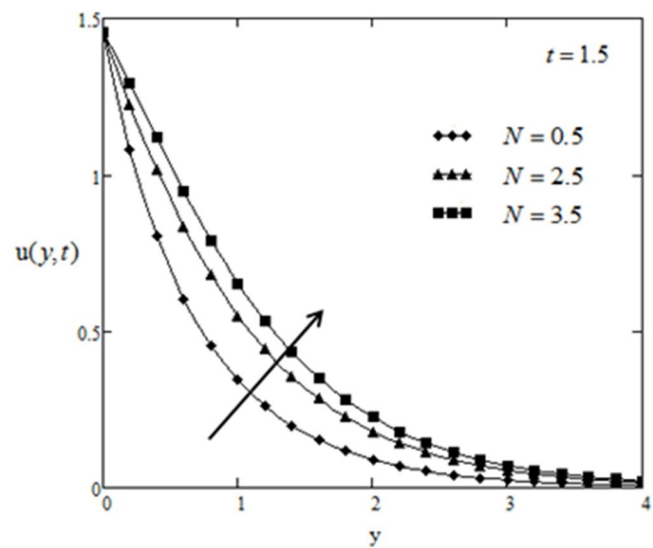


Figure 10. Velocity profile for various N when $\alpha = 0.6$, $M = 6.5$, $\Gamma = 0.2$, $Sc = 0.22$, $Pr_{eff} = 9$, $K = 3.5$ and $\gamma = 0.2$.

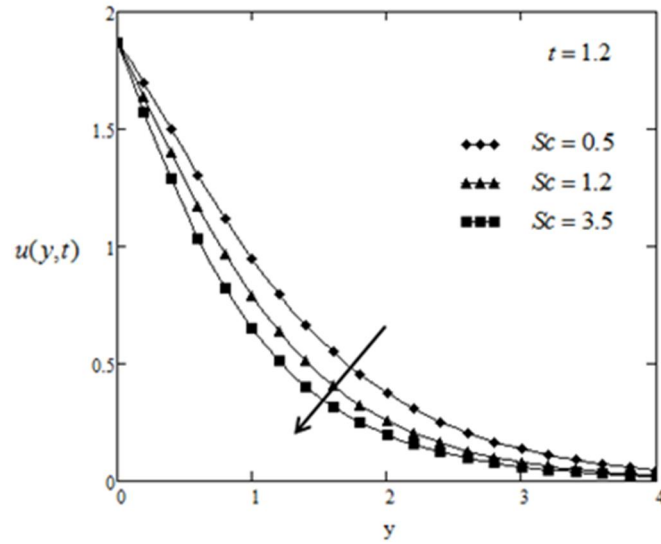


Figure 11. Velocity profile for various Sc when $\alpha = 0.2$, $M = 2.5$, $\Gamma = 0.2$, $N = 1.5$, $Pr_{eff} = 12$, $K = 2.2$ and $\gamma = 0.1$.

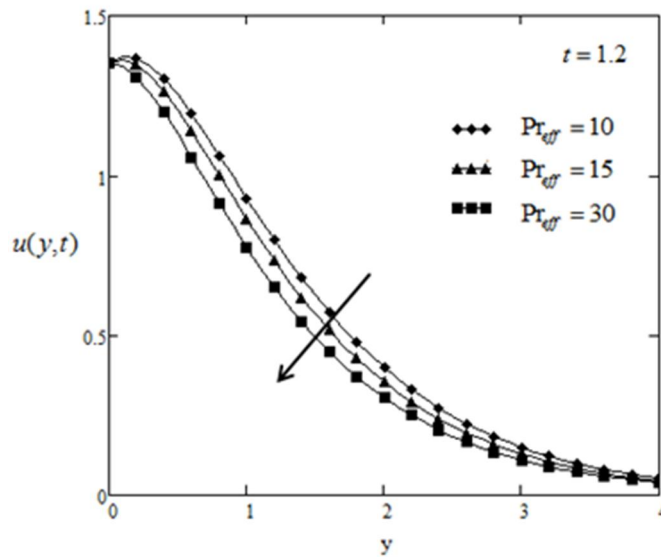


Figure 12. Velocity profile for various Pr_{eff} when $\alpha = 0.5$, $M = 0.2$, $\Gamma = 2.2$, $N = 0.7$, $Sc = 3.8$, $K = 0.5$ and $\gamma = 0.3$.

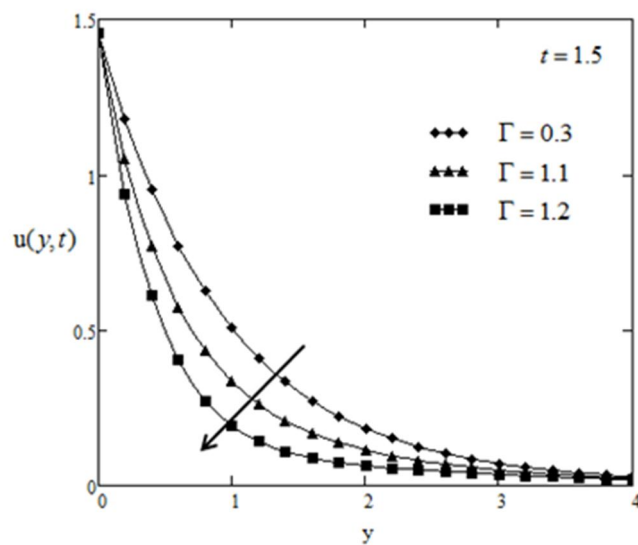


Figure 13. Velocity profile for various Γ when $\alpha = 0.2$, $M = 1.5$, $Pr_{eff} = 10$, $N = 0.5$, $Sc = 0.22$, $K = 2.5$ and $\gamma = 0.3$.

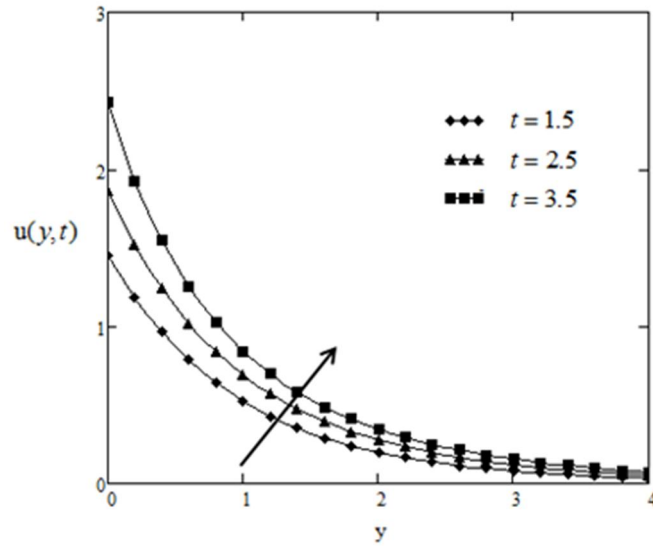


Figure 14. Velocity profile for various t when $\alpha = 0.2$, $M = 1.5$, $Pr_{eff} = 10$, $N = 0.6$, $Sc = 0.22$, $K = 2.5$, $\Gamma = 0.4$ and $\gamma = 0.3$.

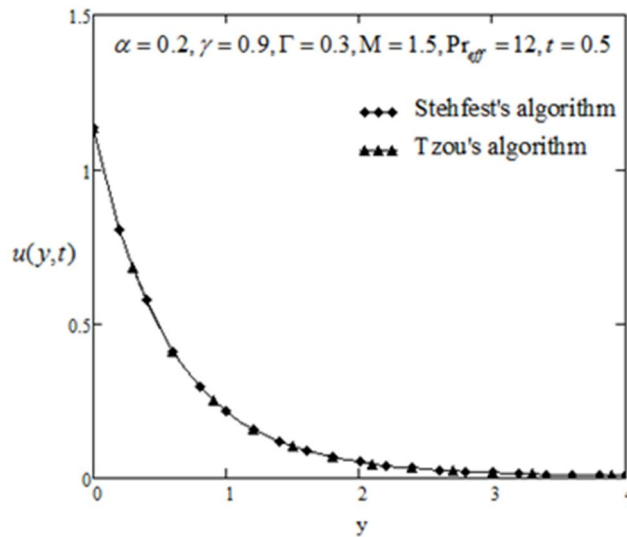


Figure 15. Velocity comparison graph when $\alpha = 0.2$, $\gamma = 0.9$, $\Gamma = 0.3$, $M = 1.5$, $Pr_{eff} = 12$ and $t = 0.5$.

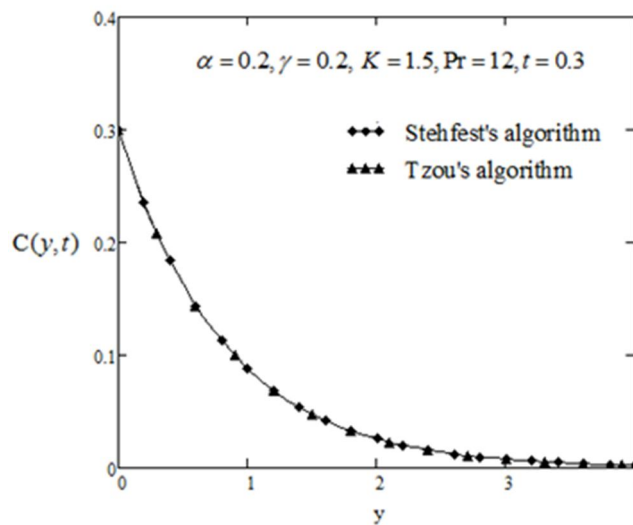


Figure 16. Concentration comparison graph when $\alpha = 0.2$, $\gamma = 0.2$, $K = 1.5$, $Pr = 12$ and $t = 0.3$.

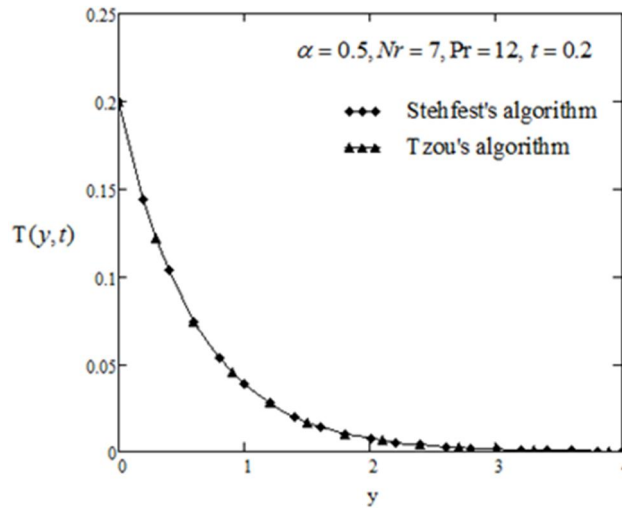


Figure 17. Temperature comparison graph when $\alpha = 0.5$, $Nr = 7$, $Pr = 12$ and $t = 0.2$.

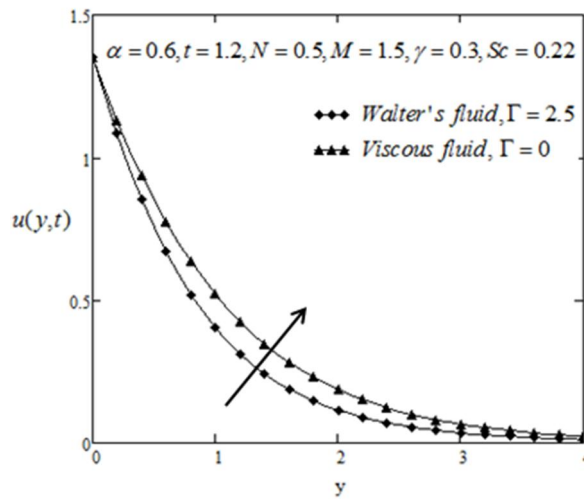


Figure 18. Velocity comparison graph of Walters'-B fluid & viscous fluid.

Tables 1–3 are made to check the effects of fractional parameter α on dimensionless temperature, velocity and concentration. The inverse Laplace transforms have been calculated numerically by using inversion algorithm, namely the Stehfest's algorithm and the Tzou's algorithm as shown in Table 4.

Table 1. Effect of fractional parameter α on dimensionless temperature when $Pr = 10$ & $Nr = 1.5$.

y	$T(y, t)$ $\alpha = 0$	$T(y, t)$ $\alpha = 0.2$	$T(y, t)$ $\alpha = 0.4$	$T(y, t)$ $\alpha = 0.6$	$T(y, t)$ $\alpha = 0.8$	$T(y, t)$ $\alpha = 1$
0	5	5	5	5	5	5
0.1	4.094	4.213	4.319	4.404	4.468	4.515
0.2	3.352	3.548	3.724	3.870	3.982	4.068
0.3	2.744	2.985	3.206	3.392	3.541	3.657
0.4	2.247	2.511	2.755	2.967	3.141	3.280
0.5	1.839	2.110	2.364	2.589	2.779	2.935
0.6	1.506	1.773	2.026	2.255	2.453	2.620
0.7	1.233	1.489	1.733	1.959	2.160	2.333
0.8	1.009	1.249	1.481	1.699	1.898	2.073
0.9	0.826	1.048	1.263	1.470	1.663	1.837
1.0	0.677	0.878	1.077	1.270	1.454	1.624

Table 2. Effect of fractional parameter α on dimensionless concentration when $K = 0.2, Sc = 2$ & $Pr = 10$.

y	$C(y, t)$	$C(y, t)$	$C(y, t)$	$C(y, t)$	$C(y, t)$	$C(y, t)$
	$\alpha = 0$	$\alpha = 0.2$	$\alpha = 0.4$	$\alpha = 0.6$	$\alpha = 0.8$	$\alpha = 1$
0	10	10	10	10	10	10
0.1	8.681	8.800	8.888	8.955	9.007	9.048
0.2	7.536	7.744	7.899	9.018	8.111	8.184
0.3	6.543	6.814	7.020	7.178	7.302	7.401
0.4	5.680	5.995	6.237	6.425	6.573	6.691
0.5	4.931	5.275	5.541	5.749	5.915	6.048
0.6	4.280	4.641	4.922	5.144	5.322	5.466
0.7	3.716	4.083	4.371	4.602	4.787	4.938
0.8	3.226	3.592	3.882	4.116	4.305	4.461
0.9	2.800	3.159	3.447	3.681	3.871	4.029
1.0	2.431	2.779	3.061	3.291	3.480	3.638

Table 3. Effect of fractional parameter α on dimensionless velocity when $Pr_{eff} = 10, t = 0.5, K = 1.5, M = 1.5$ & $Sc = 0.22$.

y	$u(y, t)$	$u(y, t)$	$u(y, t)$	$u(y, t)$	$u(y, t)$	$u(y, t)$
	$\alpha = 0$	$\alpha = 0.2$	$\alpha = 0.4$	$\alpha = 0.6$	$\alpha = 0.8$	$\alpha = 1$
0	1.134	1.134	1.134	1.134	1.134	1.134
0.1	0.946	0.956	0.966	0.975	0.983	0.991
0.2	0.789	0.807	0.823	0.838	0.852	0.965
0.3	0.659	0.681	0.701	0.720	0.737	0.754
0.4	0.551	0.575	0.597	0.619	0.638	0.657
0.5	0.461	0.486	0.510	0.532	0.553	0.573
0.6	0.387	0.412	0.435	0.457	0.479	0.499
0.7	0.325	0.349	0.372	0.394	0.415	0.435
0.8	0.274	0.297	0.318	0.339	0.359	0.379
0.9	0.231	0.252	0.273	0.293	0.312	0.330
1.0	0.196	0.215	0.234	0.253	0.271	0.288

Table 4. Validation of obtained numerical results with Tzou's algorithm.

y	Stehfest's	Tzou's	Stehfest's	Tzou's	Stehfest's	Tzou's
	$u(y, t)$	$u(y, t)$	$T(y, t)$	$T(y, t)$	$C(y, t)$	$C(y, t)$
0	1.134	1.133	0.2	0.2	0.3	0.3
0.1	0.956	0.956	0.17	0.170	0.265	0.265
0.2	0.807	0.806	0.144	0.144	0.235	0.235
0.3	0.681	0.680	0.122	0.122	0.208	0.208
0.4	0.575	0.575	0.103	0.103	0.184	0.184
0.5	0.486	0.486	0.088	0.088	0.163	0.163
0.6	0.412	0.411	0.074	0.074	0.144	0.144
0.7	0.349	0.349	0.063	0.063	0.127	0.127
0.8	0.297	0.296	0.053	0.053	0.113	0.113
0.9	0.252	0.252	0.045	0.045	0.100	0.100
1.0	0.215	0.215	0.038	0.038	0.088	0.088

5. Conclusion

The Caputo-Fabrizio fractional derivatives approach is applied to examine the unsteady MHD free convective flow of Walters'-B fluent with heat conveying analysis across an exponential isothermal upright plate engrafted in a poriferous medium. The consequent solution of the problem was obtained by applying Laplace transform method. Limiting result was extracted corresponding to Walters'-B fluid and viscid fluid. The obtained results were examined graphically likewise numerically for time fractional parameter α , effective Prandtl number, Pr_{eff} , magnetic field parameter M , permeability of porous medium K , radiation conduction parameter Nr , ratio of buoyancy forces N , Schmidt number Sc , and time t . By the following remark we conclude this article.

- 1) As the value of fractional parameter α , increases, the temperature, concentration and velocity increases.
- 2) We can see a reduction in the temperature of the fluid by enhancing the values of Prandtl number.
- 3) Increasing the value of chemical reaction K , concentration decreases and velocity of fluid lead to fall.
- 4) Concentration drop-offs by maximizing the value of Schmidt number Sc .
- 5) Velocity is a decreasing function of magnetic parameter M and chemical reaction parameter K .
- 6) As we increase the value of effective Prandtl number Pr_{eff} , as well as Walter's parameter Γ , velocity decreases.
- 7) Fractional viscid fluid shows higher velocity than fractional Walters'-B fluid.

Conflict of interest

The authors declare no conflict of interest.

References

1. Oldham K, Spanier J. *The Fractional Calculus Theory and Applications of Differentiation and Integration to Arbitrary Order*. Elsevier; 1974.
2. Samko S, Kilbas AA, Marichev O. *Fractional Integrals and Derivatives*. Taylor & Francis; 1993.
3. Du M, Wang Z, Hu H. Measuring memory with the order of fractional derivative. *Scientific Reports* 2013; 3(1). doi: 10.1038/srep03431
4. Machado JT, Mainardi F, Kiryakova V. Fractional calculus: Quo vadimus? (Where are we going?). *Fractional Calculus and Applied Analysis* 2015; 18(2): 495–526. doi: 10.1515/fca-2015-0031
5. Tenreiro Machado JA, Silva MF, Barbosa RS, et al. Some applications of fractional calculus in engineering. *Mathematical Problems in Engineering* 2010; 2010: 1–34. doi: 10.1155/2010/639801
6. Area I, Djida JD, Losada J, et al. On fractional orthonormal polynomials of a discrete variable. *Discrete Dynamics in Nature and Society* 2015; 2015: 1–7. doi: 10.1155/2015/141325
7. Area I, Losada J, Manintchap A. On some fractional Pearson equations. *Fractional Calculus and Applied Analysis* 2015; 18(5): 1164–1178. doi: 10.1515/fca-2015-0067
8. Klimek M, Odziejewicz T, Malinowska AB. Variational methods for the fractional Sturm–Liouville problem. *Journal of Mathematical Analysis and Applications* 2014; 416(1): 402–426. doi: 10.1016/j.jmaa.2014.02.009
9. Herrmann R. *Fractional Calculus: An Introduction for Physicists*. World Scientific; 2014.
10. Hilfer R. Threefold introduction to fractional derivatives. In: Klages R, Radons G, Sokolov IM (editors). *Anomalous Transport: Foundations and Applications*. Wiley-VCH Verlag; 2008. pp. 17–73. doi: 10.1002/9783527622979.ch2
11. Caputo M, Fabrizio M. A new definition of fractional derivative without singular kernel. *Progress in Fractional Differentiation & Applications* 2015; 1(2): 73–85. doi: 10.12785/pfda/010201
12. Losada J, Nieto JJ. Properties of a new fractional derivative without singular kernel. *Progress in Fractional Differentiation and Applications* 2015; 1(2): 87–92. doi: 10.12785/pfda/010202
13. Abo-Eldahab EM, Aziz MAE. Hall and ion-slip effects on MHD free convective heat generating flow past a semi-infinite vertical flat plate. *Physica Scripta* 2000; 61(3): 344–348. doi: 10.1238/physica.regular.061a00344

14. Ibrahim FS, Hassanien IA, Bakr AA. Unsteady magnetohydrodynamic micropolar fluid flow and heat transfer over a vertical porous plate through a porous medium in the presence of thermal and mass diffusion with a constant heat source. *Canadian Journal of Physics* 2004; 82(10): 775–790. doi: 10.1139/p04-021
15. Chaudhary RC, Jain A. Combined heat and mass transfer effects on MHD free convection flow past an oscillating plate embedded in porous medium. *Romanian Journal of Physics* 2007; 52(5–7): 505–524.
16. Bég OA, Bakier AY, Prasad VR. Numerical study of free convection magnetohydrodynamic heat and mass transfer from a stretching surface to a saturated porous medium with Soret and Dufour effects. *Computational Materials Science* 2009; 46(1): 57–65. doi: 10.1016/j.commatsci.2009.02.004
17. Makinde OD. Similarity solution of hydromagnetic heat and mass transfer over a vertical plate with a convective surface boundary condition. *International Journal of Physical Sciences* 2010; 5(6): 700–710.
18. Seth GS, Ansari MdS, Nandkeolyar R. MHD natural convection flow with radiative heat transfer past an impulsively moving plate with ramped wall temperature. *Heat and Mass Transfer* 2010; 47(5): 551–561. doi: 10.1007/s00231-010-0740-1
19. Khan I, Fakhar K, Shafie S. Magnetohydrodynamic free convection flow past an oscillating plate embedded in a porous medium. *Journal of the Physical Society of Japan* 2011; 80(10): 104401. doi: 10.1143/jpsj.80.104401
20. Narahari M, Debnath L. Unsteady magnetohydrodynamic free convection flow past an accelerated vertical plate with constant heat flux and heat generation or absorption. *ZAMM - Journal of Applied Mathematics and Mechanics* 2012; 93(1): 38–49. doi: 10.1002/zamm.201200008
21. Deka RK, Paul A, Chaliha A. Transient free convection flow past an accelerated vertical cylinder in a rotating fluid. *Ain Shams Engineering Journal* 2014; 5(2): 505–513. doi: 10.1016/j.asej.2013.10.002
22. Balamurugan KS, Ramaprasad JL, Varma SVK. Unsteady MHD free convective flow past a moving vertical plate with time dependent suction and chemical reaction in a slip flow regime. *Procedia Engineering* 2015; 127: 516–523. doi: 10.1016/j.proeng.2015.11.338
23. Butt AS, Ali A. Entropy generation effects in a hydromagnetic free convection flow past a vertical oscillating plate. *Journal of Applied Mechanics and Technical Physics* 2016; 57(1): 27–37. doi: 10.1134/s0021894416010053
24. Cramer KR. New from McGraw-Hill magnetofluid dynamics for engineers and applied physicists. *Electrical Engineering in Japan* 1973; 93(1): 142–142. doi: 10.1002/ej.4390930120
25. Beard DW, Walters K. Elastico-viscous boundary-layer flows I. Two-dimensional flow near a stagnation point. *Mathematical Proceedings of the Cambridge Philosophical Society* 1964; 60(3): 667–674. doi: 10.1017/s0305004100038147
26. Nandeppanavar MM, Abel MS, Tawade J. Heat transfer in a Walter's liquid B fluid over an impermeable stretching sheet with non-uniform heat source/sink and elastic deformation. *Communications in Nonlinear Science and Numerical Simulation* 2010; 15(7): 1791–1802. doi: 10.1016/j.cnsns.2009.07.009
27. Chang TB, Mehmood A, Bég OA, et al. Numerical study of transient free convective mass transfer in a Walters-B viscoelastic flow with wall suction. *Communications in Nonlinear Science and Numerical Simulation* 2011; 16(1): 216–225. doi: 10.1016/j.cnsns.2010.02.018
28. Khan I, Ali F, Shafie S, et al. Unsteady free convection flow in a Walters-B fluid and heat transfer analysis. *Bulletin of the Malaysian Mathematical Sciences Society* 2014; 37(2): 437–448.
29. Hayat T, Asad S, Mustafa M, et al. Heat transfer analysis in the flow of Walters' B fluid with a convective boundary condition. *Chinese Physics B* 2014; 23(8): 084701. doi: 10.1088/1674-1056/23/8/084701
30. Hayat T, Hutter K, Nadeem S, et al. Unsteady hydromagnetic rotating flow of a conducting second grade fluid. *Journal of Applied Mathematics and Physics* 2004; 55(4): 626–641. doi: 10.1007/s00033-004-1129-0
31. Siddheshwar PG, Mahabaleswar US. Effects of radiation and heat source on MHD flow of a viscoelastic liquid and heat transfer over a stretching sheet. *International Journal of Non-Linear Mechanics* 2005; 40(6): 807–820. doi: 10.1016/j.ijnonlinmec.2004.04.006
32. Ghasemi E, Bayat M, Bayat M. Viscoelastic MHD flow of Walters liquid B fluid and heat transfer over a non-isothermal stretching sheet. *International Journal of Physical Sciences* 2011; 6(21): 5022–5039. doi: 10.5897/IJPS11.793
33. Prakash O, Kumar D, Dwivedi YK. Heat transfer in MHD flow of dusty viscoelastic (Walters' liquid model-B) stratified fluid in porous medium under variable viscosity. *Pramana* 2012; 79(6): 1457–1470. doi: 10.1007/s12043-012-0344-z
34. Balvinder P, Krishan D, Bansal AK. Hall current effect on viscoelastic (Walter's liquid model-B) MHD oscillatory convective channel flow through a porous medium with heat radiation. *Kragujevac Journal of Science* 2014; (36): 19–32. doi: 10.5937/kgjsci1436019b
35. Ramesh K, Devakar M. Effect of Heat Transfer on the peristaltic flow of Walters B fluid in a vertical channel with an external magnetic field. *Journal of Aerospace Engineering* 2016; 29(2): 04015050. doi: 10.1061/(ASCE)AS.1943-5525.0000541

Appendix

$$L^{-1}\{e^{-y\sqrt{q}}\} = \frac{y}{2t\sqrt{\pi t}} \exp\left(-\frac{y^2}{4t}\right), L^{-1}\left\{\frac{e^{-y\sqrt{q}}}{q}\right\} = \operatorname{erfc}\left(\frac{y}{2\sqrt{t}}\right), L^{-1}\left\{\frac{e^{-y\sqrt{q+a}}}{q-b}\right\} = \psi(y, t; a, b) \quad (\text{A1})$$

$$\Psi(y, t; a, b) = \frac{e^{bt}}{2} \left[e^{-y\sqrt{a+b}} \operatorname{erfc}\left(\frac{y}{2\sqrt{t}} - \sqrt{(a+b)t}\right) + e^{y\sqrt{a+b}} \operatorname{erfc}\left(\frac{y}{2\sqrt{t}} + \sqrt{(a+b)t}\right) \right] \quad (\text{A2})$$

$$L^{-1}\{qF(q)\} = f'(t) + \delta(t)f(0) \text{ if } L^{-1}\{F(q)\} = f(t) \quad (\delta(\cdot) \text{ is the Dirac delta function}) \quad (\text{A3})$$

$$L^{-1}\left\{\frac{1}{(q+b)\sqrt{q+a}}\right\} = \frac{e^{-bt}}{\sqrt{a-b}} \operatorname{erf}(\sqrt{(a-b)t}), L^{-1}\left\{\frac{1}{\sqrt{q}}\right\} = \frac{1}{\sqrt{\pi t}} \quad (\text{A4})$$

$$L^{-1}\left\{\frac{\sqrt{q+a}}{q+b}\right\} = \frac{e^{-at}}{\sqrt{\pi t}} + \frac{1}{\sqrt{a-b}} e^{-bt} \operatorname{erf}(\sqrt{(a-b)t}) = \phi(t; a, b) \quad (\text{A5})$$

$$\int_0^t \frac{1}{\sqrt{s}} \exp\left(-\frac{y^2}{4s} - as\right) ds = \frac{\sqrt{\pi}}{2\sqrt{a}} \left\{ e^{-y\sqrt{a}} \operatorname{erfc}\left(\frac{y}{2\sqrt{t}} - \sqrt{at}\right) - e^{y\sqrt{a}} \operatorname{erfc}\left(\frac{y}{2\sqrt{t}} + \sqrt{at}\right) \right\} \quad (\text{A6})$$

$$\int_0^t \frac{1}{s\sqrt{s}} \exp\left(-\frac{y^2}{4s} - as\right) ds = \frac{\sqrt{\pi}}{y} \left\{ e^{-y\sqrt{a}} \operatorname{erfc}\left(\frac{y}{2\sqrt{t}} - \sqrt{at}\right) - e^{y\sqrt{a}} \operatorname{erfc}\left(\frac{y}{2\sqrt{t}} + \sqrt{at}\right) \right\} \quad (\text{A7})$$

$$\int_0^\infty e^{-p^2 s^2 - \frac{q^2}{s^2}} \cos\left(a^2 s^2 + \frac{b^2}{s^2}\right) ds = \frac{\sqrt{\pi}}{2^4 \sqrt{p^4 + a^4}} e^{-2c \cos(\alpha + \beta)} \cos[\alpha + 2c \sin(\alpha + \beta)] \quad (\text{A8})$$

$$\int_0^\infty e^{-p^2 s^2 - \frac{q^2}{s^2}} \sin\left(a^2 s^2 + \frac{b^2}{s^2}\right) ds = \frac{\sqrt{\pi}}{2^4 \sqrt{p^4 + a^4}} e^{-2c \cos(\alpha + \beta)} \sin[\alpha + 2c \sin(\alpha + \beta)] \quad (\text{A9})$$

where $\alpha = \frac{1}{2} \operatorname{arctg}\left(\frac{a^2}{p^2}\right)$, $\beta = \frac{1}{2} \operatorname{arctg}\left(\frac{b^2}{q^2}\right)$ and $c = \sqrt[4]{(p^4 + a^4)(q^4 + b^4)}$.

$$L^{-1}\left\{\frac{e^{-y\sqrt{\frac{Pr_{eff}s}{(1-\alpha)s+a}}}}{s}\right\} = 1 - \frac{2Pr_{eff}}{\pi} \int_0^\infty \frac{\sin\left(\frac{y}{\sqrt{1-\alpha}}x\right)}{x(Pr_{eff} + x^2)} e^{\left(\frac{-\alpha}{1-\alpha}tx^2\right)} dx \quad (\text{A10})$$

$$L^{-1}\left\{\frac{e^{-y\sqrt{\frac{s+b}{s+c}}}}{s+a}\right\} = e^{-at-y} - \frac{y\sqrt{b-c}}{2\sqrt{\pi}} \int_0^\infty \int_0^\xi \frac{e^{-a\xi}}{\sqrt{\xi}} \left(e^{a\xi - a_1\xi - \frac{y^2 Sc}{4u} - u} \right) \left(I_1\left(2\sqrt{(b-a_1)u\xi}\right) \right) d\xi du \quad (\text{A11})$$

$$G_{a,b,c}(d, t) = L^{-1}\left\{\frac{q^b}{(q^a - d)^c}\right\} \quad (\text{A12})$$

if $\operatorname{Re}(ac - b) > 0, \operatorname{Re}(q) > 0, |d| < |q^a|$

Nomenclature	Greek symbols
B magnetic field strength	β_C volumetric coefficient of expansion with concentration
C dimensional concentration in the fluid	β_T volumetric coefficient of thermal expansion
C'_w concentration of the fluid near the plate	σ electric conductivity
C'_∞ concentration of the fluid far away from the plate	k thermal conductivity of the fluid
c_p specific heat at constant pressure	ρ density
D chemical molecular diffusivity	μ coefficient of viscosity
g acceleration due to gravity	ν kinematic coefficient of viscosity
K permeability of porous medium	$\Gamma = \frac{k_o U_o^2}{\rho \nu^2}$ Walters' -B parameter
k_R Rossel and mean attenuation coefficient	
$M = \frac{\nu \sigma B_o^2}{\rho U_o^2}$ magnetic field parameter	
$N = \frac{\beta_C (C_w - C_\infty)}{\beta_T T_w}$ ratio of the buoyancy forces	
$N_r = \frac{16}{3} \frac{\sigma}{k k_R} T_\infty^3$ radiation conduction	
$Pr = \frac{\mu c_p}{k}$ Prandtl number	
$Pr_{eff} = \frac{Pr}{1+N_r}$ effective Prandtl number	
q the transform parameter	
q_r radioactive heat flux	
$Sc = \frac{\nu}{D}$ Schmidt number	
T dimensionless temperature of the fluid	
T'_w constant temperature of the plate	
T'_∞ free stream temperature	
u velocity of the fluid	
$U_o^3 = \frac{g \beta_T}{\nu} \left(\frac{k}{h} \right)^2 T_\infty$ characteristic velocity of the plate	